Regioselectivity of Radical Attacks on Substituted Olefins. Application of the SCD Model

Sason S. Shaik*,[1a] and Enric Canadell*,[1b]

Contribution from the Department of Chemistry, Ben Gurion University of the Negev, Beer Sheva 84105, Israel, and Laboratoire de Chimie Théorique,† Bâtiment 490, Université de Paris-Sud, 91405 Orsay, Cédex, France. *Received February 28, 1989*

Abstract: The SCD model is used to derive regiochemical trends in radical addition to olefins. Regiochemistry is discussed by appeal to two fundamental properties of the radical and the olefin. The first factor is the relative spin density in the $^3\pi\pi^*$ state of the olefin. Thus, *radical attack is directed toward the olefinic carbon which possesses the highest spin density.* The second factor is the relative bond strengths of the radical to the olefinic carbons. *This factor directs the regiochemistry toward the olefinic terminus which forms the strongest bond with the radical.* When the two effects join up, regioselectivity will be large, e.g., for CH_2=CHX (X = NR_2, CR, Cl, CN, Ph). When the two effects oppose one another, regioselectivity will be smaller, and regioselectivity crossovers are expected, e.g., for CF_2=CHF. The "normal" regiochemistry is shown to coincide with the spin density rule which makes identical predictions to the HOMO rule.

Radical attacks on substituted olefins[2] proceed in two regiochemical pathways. The more common result is the attack on the less substituted carbon. In some cases the common trend is reversed, and the attack proceeds on the more substituted carbon, e.g., in the reaction of CH_3 with CF_2CHF. Changing, however, the attacking radical to CF_3, CCl_3 or H restores the superiority of the "normal" pathway.[2] Also, the CH_3 radical, which reverses the common order with CF_2CHF, behaves normally with CH_2-CHF and adds to the less substituted carbon.[2a]

It is important to emphasize that the "normal pathway" generates, in many instances, the thermodynamically less stable radical.[3] In contrast, the "uncommon" attack of CH_3 on the more substituted carbon of CF_2CHF leads to the thermodynamically more stable radical CH_3CF_2CHF.[3]

Those regiochemical patterns have attracted considerable attention. Tedder[2c] and Giese[2f] have proposed a set of rules to rationalize the experimental facts. Thus, the dominant factor according to Tedder and Giese is the steric congestion of the two carbon atoms of the olefin. This dominant effect leads to the "normal" pathway of attack on the less substituted carbon. In general, though, the regiochemical outcome depends on a complex blend of bond strength, polarity, and steric effects.[2,4]

General theoretical treatments of the problem have also appeared. Thus, Bonacic-Koutecky, Koutecky, and Salem[5] have used a VB model which shows how ionic factors, which result from electronegativity differences between the attacking radical and the attacked olefinic carbon, can divert the regiochemistry to produce the less stable radical. This explanation is in line with the formulation of the polar effect by Tedder and Walton.[2a]

Canadell et al.[6] have used FMO (frontier molecular orbital) theory and argued that among the two possible orbital interactions, **1**, the SOMO-HOMO is dominant owing to the energetic proximity of the two orbitals and the reactant-like nature of the transition state which makes the three electron-three orbital interaction, **1**, a stabilizing one. This in turn means that the preferred mode of attack will occur with some expected exceptions[3,7] on the olefinic site with the highest HOMO coefficient (hereafter, the HOMO rule).

Arnaud et al.[8] and Delbecq et al.[9] have shown that the deformation energy which is required to carry the reactants to the transition state can account for the regiochemical choice. Thus, the preferred regiochemical mode of attack should be typified by a smaller deformation energy (DEF). The generality and a priori predictive ability of the DEF index has been contested, though, by Canadell et al.[3] who have shown that in the "abnormal" regiochemistry of CH_3 + CF_2CHF the preferred regiochemical pathway possesses a *larger* deformation energy. Also, the knowledge of DEF is not a priori and requires the knowlede of the transition geometry.[3,9] Nevertheless, the DEF index usually does correlate with the observed regioselectivity.

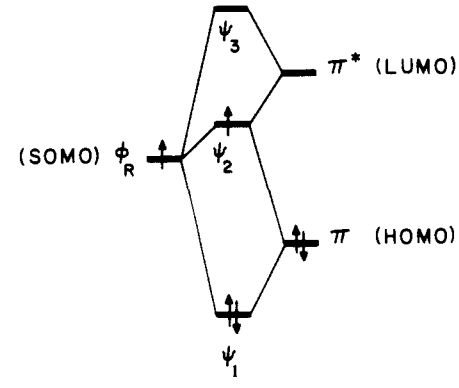

1

It is apparent that the regiochemical problem is complex and challenging. It appears that what is missing in order to conceptualize the problem clearly is a model which shows how the barrier to the reaction is formed and what are the factors which regulate the size of this barrier.

A model which directly treats the barrier and the factors which contribute to its height is the state correlation diagram (SCD)[10] approach which belongs to the general approach of curve crossing

† The Laboratoire de Chimie Thérique is associated with the CNRS (UA 506) and is a member of ICMO and IPCM (Orsay).

(1) (a) Ben Gurion University. (b) Université de Paris-Sud.

(2) (a) Tedder, J. M.; Walton, J. C. *Adv. Phys. Org. Chem.* **1978**, *16*, 51. (b) Tedder, J. M.; Walton, J. C. *Tetrahedron* **1980**, *36*, 701. (c) Tedder, J. M. *Angew. Chem., Int. Ed. Engl.* **1982**, *21*, 401. (d) Nonhebel, D. C.; Walton, J. C. *Free-Radical Chemistry*; Cambridge University Press: Cambridge, England, 1974; Chapters 7-9. (e) Beckwith, A. L. *Tetrahedron* **1981**, *37*, 3073. (f) Giese, B. *Angew. Chem., Int. Ed. Engl.* **1983**, *22*, 753.

(3) Canadell, E.; Eisenstein, O.; Ohanessian, G.; Poblet, J. M. *J. Phys. Chem.* **1985**, *89*, 4856.

(4) Münger, K.; Fischer, H. *Int. J. Chem. Kinet.* **1985**, *17*, 809.

(5) Bonacic-Koutecky, V.; Koutecky, J.; Salem, L. *J. Am. Chem. Soc.* **1977**, *99*, 842.

(6) Poblet, J. M.; Canadell, E.; Sordo, T. *Can. J. Chem.* **1983**, *61*, 2068.

(7) Canadell, E.; Igual, J. *J. Chem. Soc., Perkin Trans. 2* **1985**, 1331.

(8) (a) Arnaud, R.; Ellinger, Y.; Subra, R.; Douady, J. *Theochem.* **1984**, *110*, 203. (b) Arnaud, R.; Barone, V.; Olivella, S.; Russo, N.; Solé, A. *J. Chem. Soc., Chem. Commun.* **1985**, 1331. (c) Arnaud, R.; Subra, R.; Barone, V.; Lelj, F.; Olivella, S.; Solé, A.; Russo, N. *J. Chem. Soc., Perkin Trans. 2* **1986**, 1517.

(9) Delbecq, F.; Ilavsky, D.; Anh, N. T.; Lefour, J. M. *J. Am. Chem. Soc.* **1985**, *107*, 1623.

(10) (a) Shaik, S. S. *J. Am. Chem. Soc.* **1981**, *103*, 3692. (b) Shaik, S. S. *Prog. Phys. Org. Chem.* **1985**, *15*, 197. (c) Shaik, S. S. In *New Concepts for Understanding Organic Reactions*; Bertran, J., Csizmadia, I. G., Eds.; NATO ASI Series, Reidel: Dordrecht, 1989; Vol. 267.

0002-7863/90/1512-1446$02.50/0

diagrams.[11-14] The SCD model has already been applied qualitatively to a variety of reactions.[10b,15,16] Recently, a few groups have shown that these kinds of diagrams can be rigorously and meaningfully defined on the "state of the art" level of computations.[17]

Previous modelling, of the barrier in radical reactions, in terms of curve crossing diagrams have been presented recently by Shaik and co-workers,[18] by Pross,[19] and by Klessinger and Höweler.[20] This paper utilizes the SCD model[10,15,18] to derive the barrier controlling factors and applies them to the understanding of the regiochemical patterns in radical addition to olefins. Our goal is not to invoke new effects but rather to unify and show how the various effects follow naturally from a single model of the activation process and what are the major effects which determine the regiochemistry.

I. The SCD Model. The Barrier Controlling Factors

Any chemical step (R (reactant) → P (product)) which involves bond interchange has reactants and products which possess distinct spin-pairing schemes. For radical addition to olefins the spin pairs are shown in **2a** vs **2b**. Thus, in **2a** the spins are paired across

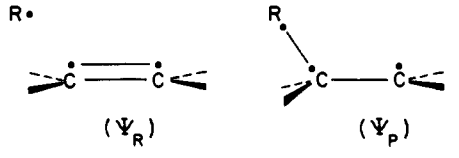

2a **2b**

the olefinic carbons, as shown by the line connecting the two heavy dots which symbolize electrons. The third electron on R is decoupled from the other two, and there exists a repulsive interaction between the single electron and the electron pair, owing to a dominant triplet relationship between the respective spins.[18a,d] Conversely, the spins in **2b** are paired up across the R—C linkage, and there exists a predominant triplet spin relationship between each of these spin-paired electrons and the odd electron on the terminal carbon.[18a,d]

The SCD in Figure 1 shows that the transformation of Ψ_R to Ψ_P takes place via the involvement of two excited states.[10] Each excited state (or pseudostates[18c,d]) of the diagram has the same spin-pairing pattern as the ground state in the end of the correlation line. For the radical addition to an olefin, the excited states

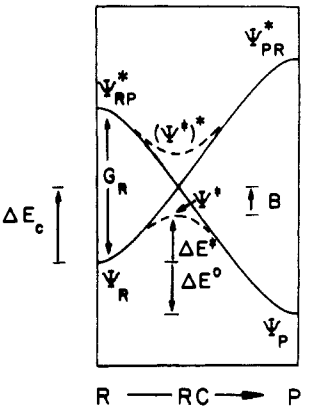

Figure 1. SCD for a chemical step, R → P. The avoided crossing is shown by dashes. The Ψ^* is the transition state for the R → P reaction with a barrier ΔE^*. The barrier is given as $\Delta E^* = \Delta E_c - B$ where ΔE_c is the height of the crossing point relative to the reactants, and B is the quantum mechanical resonance energy (in absolute value). G_R is the diagram gap and corresponds to a specific electronic excitation of the reactants, which is a $^3\pi\pi^*$ excitation for radical addition to olefins.

involve triplet excitation of *the bond* in the respective ground state and spin pairing of the two electrons across the long linkage. For example, the Ψ_R and $\Psi^{\bullet}_{RP}$ pair are schematized in **3a** vs **3b**. One can see that Ψ_R in **3a** involves spin pairing of the π-bond in the olefin, whereas $\Psi^{\bullet}_{RP}$ in **3b** involves a triplet relationship in the same bond and spin pairing across the infinitely long R—C linkage. The arrows in each case indicate the linkage, which has the triplet relationship. Thus, $\Psi^{\bullet}_{RP}$ differs from Ψ_R by a singlet-to-triplet $\pi\pi^*$ excitation. Symmetric types of arguments exist for the other pair of states, Ψ_P and $\Psi^{\bullet}_{PR}$ in Figure 1.

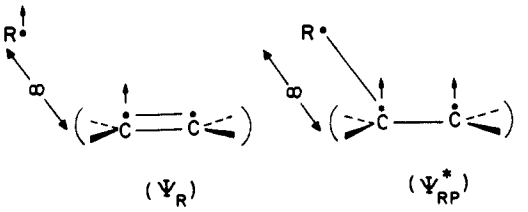

3a **3b**

Let us now consider the behavior of these states along the reaction coordinate of Figure 1 and use $\Psi^{\bullet}_{RP}$ and Ψ_R as examples. As can be seen from **3b**, $\Psi^{\bullet}_{RP}$ will be stabilized as R approaches the olefin and as the olefin undergoes C–C bond elongation and pyramidalization of its trigonal centers. The first effect is dominant because, by the R-olefin approach, the spin pair in **3b** becomes a bond which greatly stabilizes $\Psi^{\bullet}_{RP}$. Bond elongation and pyramidalization are also important, as the triplet $\pi\pi^*$ state of ethylene is known to be stabilized by these distortions.[21] The two effects together stabilize $\Psi^{\bullet}_{RP}$ until it becomes Ψ_P (Figure 1).

Along the same reaction coordinate, Ψ_R(**3a**) is destabilized. Firstly, the R-olefin approach results in exchange repulsion due to the triplet relationship. Secondly, bond elongation and pyramidalization of the olefin are also costly, because ground-state olefins are destabilized by these distortions. There are other interactions which temper the rise of Ψ_R along the reaction coordinate.[10b] These are inter- and intramolecular electrostatic interactions and polarization.[2,3,9] Conversely, steric effects will accentuate the rise of Ψ_R.[10b] In any case, the exchange repulsion and bond distortion dominate the behavior of Ψ_R which rises and eventually correlates to $\Psi^{\bullet}_{PR}$ (Figure 1).

Thus, the curve crossing in Figure 1 is simply the mechanism of electronic and bond reorganization which occurs during the transformation.[10] At the crossing point, there exist two localized bonding wave functions (of reactants and product) which are degenerate, that is, in "resonance". These two wave functions mix

(11) For an early curve crossing model, see: Evans, M. G.; Polanyi, M. *Trans. Faraday Soc.* **1936**, *32*, 1340. Bell, R. P. *Proc. Roy. Soc. London* **1936**, *A154*, 414.

(12) For VBCM curve crossing diagrams, see: (a) Pross, A.; Shaik, S. S. *Acc. Chem. Res.* **1983**, *16*, 363. (b) Pross, A. *Adv. Phys. Org. Chem.* **1985**, *21*, 99.

(13) For curve crossing diagrams generated with empirical VB theory, see: Warshel, A.; Weiss, R. M. *J. Am. Chem. Soc.* **1980**, *102*, 6216.

(14) For a general analysis of curve crossings, see: (a) Salem, L. *Science (Washington, D.C.)* **1976**, *191*, 822. (b) Salem, L.; Leforestier, C.; Segal, G.; Wetmore, R. *J. Am. Chem. Soc.* **1975**, *97*, 479.

(15) (a) Shaik, S. S. *J. Org. Chem.* **1987**, *52*, 1563. (b) Cohen, D.; Bar, R.; Shaik, S. S. *J. Am. Chem. Soc.* **1986**, *108*, 231. (c) Buncel, E.; Shaik, S. S.; Um, I.-H.; Wolfe, S. *J. Am. Chem. Soc.* **1988**, *110*, 1275.

(16) (a) Williams, I. H. *Bull. Soc. Chim. (Fr.)* **1988**, 192. (b) Hammond, R. B.; Williams, I. H. *J. Chem. Soc., Perkin Trans. 2* **1989**, 59.

(17) (a) Bernardi, F.; Robb, M. A. *J. Am. Chem. Soc.* **1984**, *106*, 54. (b) Bernardi, F.; Olivucci, M.; McDouall, J. J. W.; Robb, M. A. *J. Am. Chem. Soc.* **1987**, *109*, 544. (c) Robb, M. A.; Bernardi, F. In *New Concepts for Understanding Organic Reactions*; Bertran, J., Csizmadia, I. G., Eds.; NATO ASI Series, Reidel: Dordrecht, 1989; Vol. 267. (d) Sevin, A.; Hiberty, P. C.; Lefour, J. M. *J. Am. Chem. Soc.* **1987**, *109*, 1845. (e) Maitre, P.; Ohanessian, G.; Shaik, S. S.; Hiberty, P. C. *J. Phys. Chem.* In press. (f) Sini, G.; Hiberty, P. C.; Shaik, S. S.; Ohanessian, G.; Lefour, J. M. *J. Phys. Chem.* In press. (g) Kabbaj, O. K.; Volatron, F.; Malrieu, J. P. *Chem. Phys. Lett.* **1988**, *147*, 353.

(18) (a) Shaik, S. S.; Bar, R. *Nouv. J. Chim.* **1984**, *8*, 11. (b) Shaik, S. S.; Hiberty, P. C. *J. Am. Chem. Soc.* **1985**, *107*, 3089. (c) Shaik, S. S.; Hiberty, P. C.; Ohanessian, G.; Lefour, J. M. *Nouv. J. Chim.* **1985**, *9*, 385. (d) Shaik, S. S.; Hiberty, P. C.; Lefour, J. M.; Ohanessian, G. *J. Am. Chem. Soc.* **1987**, *109*, 363.

(19) Pross, A. *Isr. J. Chem.* **1985**, *26*, 390.

(20) Klessinger, M.; Höweler, U. *Croat. Chem. Acta* **1986**, *59*, 653.

(21) Volland, V. W.; Davidson, E. R.; Borden, W. T. *J. Am. Chem. Soc.* **1979**, *101*, 533.

and generate two new states, the lower of which is the transition state, $\Psi^{\ddagger}$. Thus, the avoided crossing interaction B is the quantum mechanical resonance energy of the transition state.[15a,18d] Indeed, in the transition state there is delocalization of the three electrons (shown in **3**) over the three reaction centers much the same as the three π-electrons of allyl radical.[10c,18,22] The transition state is therefore a unique point on the reaction profile. It is at this point where electrons become delocalized, so that beyond and before it the bonds can be interchanged.[10]

The Mechanism of Activation.[10b,c,15a,b] The origins of the barrier can be formulated now in light of the above analysis. The transition state occurs by avoided crossing of a ground state (e.g., Ψ_R) and its excited state (e.g., Ψ^{*}_{RP}) which are in resonance at the crossing point of Figure 1. The height of the crossing point, ΔE_c in Figure 1, is accordingly the bond distortion and intermolecular repulsive energies by which Ψ_R has to be *raised* to achieve resonance with Ψ^{*}_{RP}. At the same time the height of the crossing point is, per definition, a fraction (f) of the gap (G_R) that has to be overcome.[10b,c] We may then write ΔE_c as follows:

$$\Delta E_c = \Delta E_{dis} + \Delta E_{rep} = fG_R; \qquad G_R = \Delta E_{ST}(\pi\pi^*) \quad (1)$$

Here ΔE_{dis} is the distortion energy and ΔE_{rep} is the net intermolecular repulsive energy. $\Delta E_{ST}(\pi\pi^*)$ is the singlet-to-triplet $\pi\pi^*$ excitation energy of the olefin.[18a] Thus, the barrier for radical addition to olefin may be written simply as eq 2, where B is the absolute value of the quantum mechanical resonance energy.

$$\Delta E^{\ddagger} = fG_R - B \quad (2)$$

$$fG_R = \Delta E_C = \Delta E_{dis} + \Delta E_{rep}$$

$$G_R = \Delta E_{ST}(\pi\pi^*)$$

By use of simplified versions of VB theory[10c,22] it is possible to deduce that the B quantity is proportional to the sum of the bond energies[23] in the transition state, that is eq 3,

$$B \propto (D^{\ddagger}_{RC} + D^{\ddagger}_{\pi}) \quad (3)$$

where $D^{\ddagger}$ represents the bond energy in the TS geometry. In a structurally related series there is a trade-off of bond strengths so that B will be a quasi-constant quantity (this is equivalent to saying that there is conservation of the total bond order in such series[24]). Indeed, as we shall see later on, the variation of B is not dominant, and it can be assumed constant in qualitative reasonings with eq 2.

It follows, therefore, that in order to understand the variation in the barrier, it is sufficient to discuss the variations of the ΔE_c term in eq 2. Consider two reactions which possess the same gap G_R and differ only in their reactions ergonicity ($\Delta E°$). In this case ΔE_c is reduced as $\Delta E°$ becomes more negative (more exergonic). This is schematized in **4a** vs **4b** which show that the net effect of increasing exergonicity is the decrease of the f factor. If the avoided crossing interaction does not vary in an opposing manner, we obtain the well-known Bell–Evans–Polanyi principle.[11]

The reaction exergonicity for a radical addition reaction depends on the bond energy (D) difference between the R–C bond in the

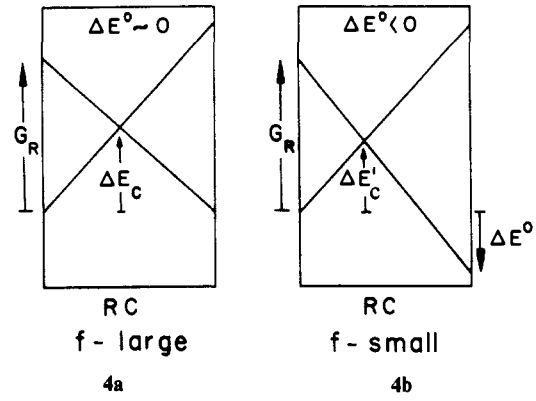

4a **4b**

product radical and the π-bond in the olefin that is

$$\Delta E° = D_{R-C} - D_{\pi} \quad (4)$$

Thus, the stronger the bond which the radical makes with carbon the more exergonic the reaction. In some cases, polar bonds tend to be also stronger bonds, so that part of the "polar effect"[2a] is a thermodynamic effect of bond strength.[5]

Consider now two reactions which possess the same exergonity but differ only in their energy gaps G_R. Then as depicted in **5a** vs **5b** the larger the gap the higher is ΔE_c. If again, B does not

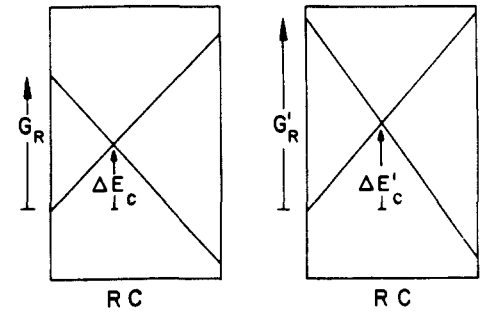

5a **5b**

change in the opposite manner, we obtain the *energy gap-rule*,[15a,18a,d] that the reaction barrier decreases as G_R decreases. In radical additions, the gap G_R is simply the singlet-to-triplet $\pi\pi^*$ excitation energy of the olefin (see eq 1).

Finally, consider the two reactions which possess the same gaps and reaction exergonicities. In this case, the relative ΔE_c values will depend on the curvatures of descent of the curves.[10b] Drawings **6a** vs **6b** illustrate such two cases. Thus, in **6a** Ψ^{*}_{RP} descends steeply toward the crossing point, while in **6b** Ψ^{*}_{RP} descends in a sluggish manner. The result is that a higher crossing point is obtained for **6b**. Since the gap is constant then this means also a higher f for **6b** vs **6a** (recall, $f = \Delta E_c/G_R$ in eq 1).

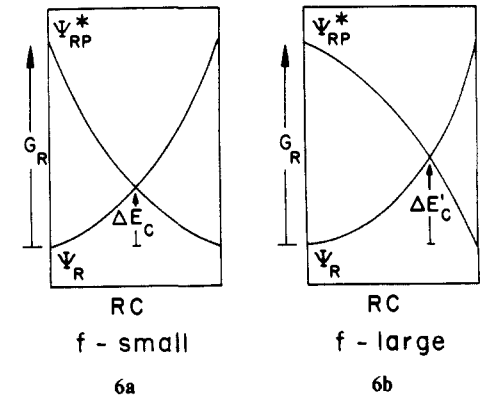

6a **6b**

To associate the curve's slope with some chemical property which possesses a predictive value, we recall that Ψ^{*}_{RP} (in **3b**) descends in energy because the two spin-paired electrons are gradually coupled in a new R–C bond. The magnitude of the bond-coupling interaction depends, in turn, on the probability of

(22) Malrieu, J. P. *Nouv. J. Chim.* **1986**, *10*, 61.

(23) (a) By using the appendix in ref 10c, B becomes

$$B = A(2h_{RC}s_{RC} + 2h_{\pi}s_{\pi})$$

$$A = 1/(4 + 3s^2_{RC} + 3s^2_{\pi} + s^4_{RC} + s^4_{\pi})$$

where h is the effective resonance integral between the hybrids of atomic orbitals of the reaction centers of the transition state, and s is the corresponding overlap. Since a $2hs$ term is the expression for the bond energy in VB theory (ref 23b below), there follows eq 3 in the text. (b) $2hs$ is the Heitler–London bond energy: Heitler, W.; London, F. *Z. Phys.* **1927**, *44*, 455. The same quantity is denoted by J (the exchange interaction) in most textbooks. For an illuminating discussion, see: McWeeny, R.; Sutcliffe, B. T. *Methods of Molecular Quantum Mechanics*; Academic Press: London, 1969; Chapter 6.

(24) See, for example: Wolfe, S.; Mitchell, D. J.; Schlegel, H. B. *J. Am. Chem. Soc.* **1981**, *103*, 7692.

having odd electron density directly on the union centers, those centers which form the new R–C bond. The smaller the odd electron density on these union centers, the weaker the bond-coupling interaction and vice versa. Thus, a major property which affects the curve's slope derives from the delocalization properties of the R• and the triplet Ċ–Ċ components of $\Psi^{\bullet}_{RP}$. Whenever either one of these components possesses substituents which reduce, by delocalization, the odd electron density on the union centers, the net outcome will be a reduction of the bond-coupling interaction and a shallow slope as illustrated in **6b**. This will in turn mean that, for a given triplet energy gap, the ground-state Ψ_R will have to undergo greater destabilization to achieve resonance with $\Psi^{\bullet}_{RP}$. Greater destabilization means according to eq 2 greater distortion and intermolecular repulsion, with due implications on the structure of the transition state. The slope of the curves depends on the various interactions along the reaction coordinate.[10b] The rate of change of these interactions, along the reaction coordinate, determines the slope of descent of $\Psi^{\bullet}_{RP}$ and of ascent of Ψ_R. One can therefore envision other curvature factors[10b,15b] that affect the value of f (for a given G_R in eq 2); for example, steric effects will raise the ascent of Ψ_R and cause a similar effect of the electron delocalization. We cannot make any decisive statements as to which of the factors will be dominant in a given situation. We can however draw judgement for two extreme situations. If the olefin substituents are not large (e.g., heteroatoms, CH_3, vinyl, CN, etc.), the electron delocalization effect will be dominant, as it is concerned with strong interactions of chemical bonding. If, however, there are bulky substituents (e.g., tBu), the steric effects will add their influence on the slope factors.

II. Factors of Regioselectivity

In a regiochemical problem, the two pathways have the same gap, G_R (Figure 1) in the SCD, because we are starting with the same two reactants. Therefore, in principle, the regiochemical factors can be (i) different slope (**6a** vs **6b**) effects and (ii) different reaction exergonicities, $\Delta E°$ (**4a** vs **4b**).

The first factor is the curvature effect which, for a given attacking radical, is associated with electron delocalization in the triplet state of the olefin. In the case of ethylene, the triplet state, $^3\pi\pi^*$, involves one odd electron on each carbon. A substituent will introduce inequality of the spin density on the two olefinic carbons. This inequality will introduce a *regiochemical preference of attack on the site of the highest spin density.*

The spin density in the triplet state of a substituted olefin can be predicted by use of simple VB arguments, based on resonance theory. Consider a substituent X which possesses a lone pair (e.g., X = F, Cl, OR, etc.) or an X which can donate an electron pair in conjugation (e.g., CH_3, etc.). The $^3\pi\pi^*$ state can be described as a resonance hybrid of two forms in **7a**. The principal form

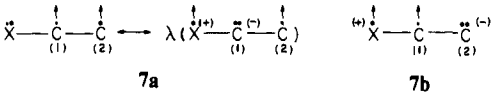

7a **7b**

(left) is purely covalent, and the secondary form (right, $\lambda < 1$) is zwitterionic. There is yet another zwitterionic structure, **7b**. This structure keeps the mutually repulsive triplet electrons adjacent to each other and weakens the stabilizing electrostatic interaction by separating the charges. On the other hand, the zwitterionic form of **7a** minimizes the triplet interaction and maximizes the electrostatic interaction. Therefore **7b** is less important and is not considered in **7a**. Similar arguments, for other cases, can show that regardless of the nature of X, its net effect is to take up spin density and to increase it thereby on C_2 at the expense of C_1.[25] The qualitative spin density distribution in the $^3\pi\pi^*$ state is summarized in **8** where the sizes of the arrows indicate the relative spin density. The same analysis can be done more formally, by projecting the VB contributions[26] from the MO

(25) See, for example, the major VB structure of triplet butadiene: Bonacic-Koutecky, V.; Ishimaru, S. *J. Am. Chem. Soc.* **1977**, *99*, 8134.
(26) Hiberty, P. C.; Leforestier, C. *J. Am. Chem. Soc.* **1978**, *100*, 2012.

Table I. Spin Densities in the $^3\pi\pi^*$ State of Olefins and Their HOMO Coefficients

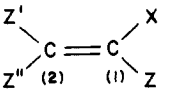

entry	olefin: substituents on C1	olefin: substituents on C2	spin densities[a] C1	spin densities[a] C2	HOMO coefficients[b] C1	HOMO coefficients[b] C2
1	F, H	H, H	1.083	1.231	0.5208	0.6470
2	F, F	H, H	0.984	1.218	0.4706	0.6744
3	F, F	F, H	0.990	1.075	0.5021	0.5810
4	Cl, H	H, H	1.144	1.231	0.5055	0.5722
5	F, F	Cl, H	0.991	1.135	0.4516	0.5865
6	CH_3, H	H, H	1.216	1.232	0.6025	0.6427
7	CF_3, H	H, H	1.191	1.227	0.6338	0.6167
					0.6114[c]	0.6430[c]
8	CN, H	H, H			0.5267	0.5537
9	$HC{=}CH_2$, H	H, H	0.104	1.107	0.4005	0.5288

[a] 3-21G calculations with standard geometries [b] STO-3G coefficients. [c] Extended Hückel coefficients.

wave function of the $^3\pi\pi^*$ state. The qualitative conclusions are in accord with the description in **8**. Furthermore, the formal

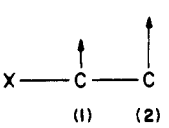

8

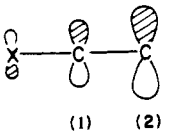

9

analysis shows that the relative spin densities coincide usually with the relative sizes of the AO coefficients of the π orbital which is the HOMO of the olefin. Thus, in most cases the HOMO has a higher coefficient on the unsubstituted carbon, C_2, as depicted in **9**, e.g., X = F, Cl, and so on.[6]

To test our qualitative reasonings we have performed 3-21G calculations of spin densities in the $^3\pi\pi^*$ states on a variety of olefins. These are presented in Table I alongside the coefficients of the HOMO calculated with STO-3G (unless indicated otherwise). It can be seen that (a) the spin density is uniformly larger at the *less* substituted carbon (C_2) and (b) the relative size of the HOMO coefficients coincides with the relative size of the spin densities, with one exception where extended Hückel and STO-3G give opposite trends of coefficient sizes.

Let us now consider the effect of spin density distribution on the regiochemistry. As discussed in **6a** vs **6b**, less odd electron density on the site of attack will cause a shallow descent of the excited state, $\Psi^{\bullet}_{RP}$, and a higher crossing point will result. A clear statement can be made that, *in the absence of opposing effects, the preferred site of attack on the olefin will be the less substituted site which possesses the highest spin density in the triplet state ($^3\pi\pi^*$) of the olefin.* Since HOMO density coincides with triplet spin density, the preceding statement coincides with the HOMO rule of Canadell et al.[6]

Let us clarify this point further by appealing to **6a** vs **6b**. Consider then the attack on the site of higher spin density, C_2. Here the bond-coupling interaction in $\Psi^{\bullet}_{RP}$ is strong early on, and the descent of $\Psi^{\bullet}_{RP}$ is therefore steep, as in **6a**. This will require Ψ_R to invest less distortion and less intermolecular repulsion in order to achieve resonance with $\Psi^{\bullet}_{RP}$. This in turn means that *in the TS the olefin will be less deformed and the distance between the radical and the olefin will be large.* Conversely, during the attack on the spin-poor site C_1, the descent of $\Psi^{\bullet}_{RP}$ is sluggish as in **6b** because the smaller spin density on C_1 weakens the bond-coupling interaction (in $\Psi^{\bullet}_{RP}$). This will now require Ψ_R to be raised more in energy in order to achieve crossing with $\Psi^{\bullet}_{RP}$. Since energy raising of Ψ_R means more distortion (ΔE_{dis}) and intermolecular repulsion (ΔE_{rep}, eq 2), this will also mean that *at the TS which corresponds to the attack on the spin-poor site, the olefin will now be more deformed with a shorter distance between the radical and the olefin.*

The reactions of fluoroethylene with CH_3 can serve as examples for the effect of the spin density (or HOMO coefficient). Ab initio calculations by Canadell et al.,[6] with the 3-21G basis set, indicate that the regiochemical pathways differ marginally in their reaction ergonicities (ΔE° = −23.0, −24.3 kcal/mol, and the small difference favors the substituted site, see **10**). Thus, we can refer to this case as one where ΔE° is constant for the two pathways in the same sense of **6a** vs **6b**.

The ΔE_c and B quantities which are required for the discussion (see eq 2) are shown in **10a** vs **10b** (in kcal/mol). These quantities

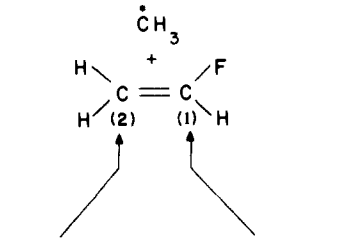

10a	**10b**
$\Delta E^\ddagger$ = 7.7	$\Delta E^\ddagger$ = 8.6
ΔE_c = 29.9	ΔE_c = 33.2
B = 22.2	B = 24.7
ΔE_{dis} = 6.7	ΔE_{dis} = 8.8
ΔE_{rep} = 23.2	ΔE_{rep} = 24.4
ΔE° = −23.0	ΔE° = −24.3

can be derived at the SCF level from a standard Morokuma analysis.[27] Thus, the ΔE_c term is the sum of the DEF, EX, ES, and PL terms in the Morokuma scheme. The ΔE_c term gives the total energy of the localized reactant (Ψ_R) at the crossing point. The B term is the difference between the SCF energy of the TS and the localized reactant at the TS.[18d] In terms of the Morokuma scheme B is simply the sum of MIX and CT. Shown in **10** also are the components of ΔE_c which are ΔE_{dis} (i.e., DEF) and ΔE_{rep} (i.e., EX + ES + PL).

As may be seen from **10a** vs **10b**, the higher barrier corresponds to the attack on the substituted carbon, **10b**, which is the site of lower spin density and HOMO coefficient. In accord, we can see that the crossing point for this case is higher in energy than in **10a**. The breakdown of ΔE_c into its components shows that the attack on the spin-poor site, **10b**, requires higher olefin distortion, ΔE_{dis}, and also higher intermolecular repulsion, ΔE_{rep}.

The geometries of the corresponding TS's show that the higher ΔE_{dis} in **10b** coincides with a more deformed olefin, while the higher ΔE_{rep} coincides with a shorter distance between the radical and the olefin, as depicted in the TS schemes in **11a** vs **11b**.[3] Similar trends in the structure of the TS have been reported for H + CH_2CHCl by Schlegel and Sosa.[28] These results are in good agreement with our preceding analysis and would have not been easily *anticipated* from a steric argument alone.

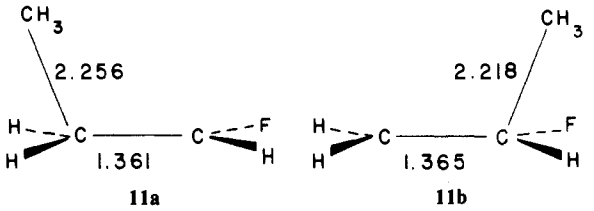

11a **11b**

Before we move on to other effects, it is worthwhile to note that the value of B in **10a** and **10b** is not a constant but is, in fact, larger for the regiochemically inferior pathway. This is a result of the shorter bond length to the radical, **11b**. There is thus a compensation mechanism so that transition states which require more distortion and repulsion to be generated acquire also higher quantum mechanical resonance energies. This trend is observed in most of the transition states to follow.

(27) Kitaura, K.; Morokuma, K. *Int. J. Quantum Chem.* **1976**, *10*, 325.
(28) Schlegel, H. B.; Sosa, C. *J. Phys. Chem.* **1984**, *88*, 1141.

Since the effect of B opposes the effect of ΔE_c, this may cause problems in making predictions. Fortunately in the problems discussed in this paper, the variation of B is smaller than the variation in ΔE_c, and the regiochemistry is dominated by the distortion and repulsive energies which are required in order to promote crossing between Ψ_R and Ψ^*_{RP}.

Let us now consider the effect of ΔE° by appeal to **4a** vs **4b**. This effect will be contributed by (a) the differences in the bond energies (D) of the two possible radical products, e.g., **12** (this effect should not be confused with the triplet density effect which is related to the bond-coupling interaction at the initial stages along the reaction coordinate), and (b) the different stabilizing or destabilizing interaction of the radical center in the product, **12**. If

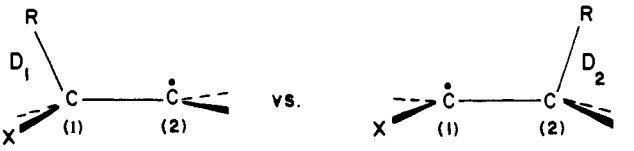

a vs. b

12

we focus on the bond strength effect, we can distinguish two kinds of substituents: those which weaken the adjacent C–R bond in **12a** and those which strengthen it. Substituents of the first type are electron donors like NR_2, Cl, OR, and CH_3 or electron acceptors, e.g., CN, and electron conjugators, e.g., Ph, $HC{=}CH_2$.[29] A substituent of the second type is fluorine which normally strengthens the bond adjacent to it.[29d,e] All the substituents of the first kind, e.g., X = NR_2, Cl, CH_3, Ph, CN, $HC{=}CH_2$, will give more exergonic reactions for attack on C_2, **12b**, while X = F will usually give more exergonic reactions for attack on C_1.

We can see then that for X's of the first kind, e.g., X = NR_2, Cl, CH_3, etc., the ΔE° effect can join the spin-density effect to direct the regiochemistry to C_2. On the other hand, for X = F, the C_2 regiochemical direction which is affected by the spin-density effect will be opposed by the ΔE° effect. Let us discuss the two situations separately.

The results of the 3-21G study of Delbecq et al.[9] are shown in **13a** vs **13b**. It is seen that ΔE° is more exergenic for the attack on C_2 and that this site has in addition a higher spin density in the triplet state. The combination of the two effects leads to a much lower energy crossing point, ΔE_c (**13a**) at C_2. As discussed

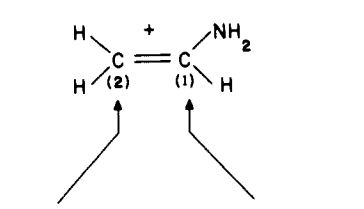

13a	**13b**
$\Delta E^\ddagger$ = 3.4	$\Delta E^\ddagger$ = 6.7
ΔE_c = 14.9	ΔE_c = 24.0
B = 11.5	B = 17.3
ΔE_{dis} = 1.9	ΔE_{dis} = 5.3
ΔE_{rep} = 13.0	ΔE_{rep} = 18.7
ΔE° = −39.8	ΔE° = −31.4

above, this is seen to correspond to a smaller ΔE_{dis} and ΔE_{rep} for **13a** relative to **13b**. This, in turn, means that considerably less

(29) See, for example: (a) Burkey, T. J.; Castelhano, A. L.; Griller, D.; Lossing, F. P. *J. Am. Chem. Soc.* **1983**, *105*, 4701. (b) Holmes, J. L.; Lossing, F. P. *Int. J. Mass Spectrom. Ion Process* **1984**, *58*, 113. (c) Holmes, J. L.; Lossing, F. P.; Terlouw, J. K. *J. Am. Chem. Soc.* **1986**, *108*, 1086. (d) Wu, E.-C.; Rodgers, A. S. *J. Am. Chem. Soc.* **1976**, *98*, 6112. (e) Kerr, J. A.; Parsonage, M. J.; Trotman-Dickenson, *Handbook of Chemistry and Physics*; CRC Press: Cleveland, OH, 1976; pp F-204–F-220.

olefin distortion and less H–olefin approach are required in order to achieve crossing for the C_2 attack relative to the C_1 attack. This is indeed manifested in the structures of the TS's as reported by Delbecq et al.[9] We emphasize that the differences in both the ΔE_c quantities and the geometric features of the TS are much larger than in the case of fluoroethylene (**10**, **11**) where only spin-density effects direct the regiochemistry.

Let us further inspect the competition of the two effects by appeal to the computational results for $H_2C=CF_2 + CH_3$. Using Table I, it is seen that the spin-density effect is larger for $CH_2=CF_2$ than for $CH_2=CHF$. Despite this larger effect the computed regiochemical preference for C_2 is approximately equal for $CH_2=CF_2$ and $CH_2=CHF$ by use of either 3-21G or 4-31G[8b,c] calculations. The root cause is seen to be $\Delta E°$ as shown in **14a** vs **14b** where the 4-31G results by Olivella et al.[8b,c] have been

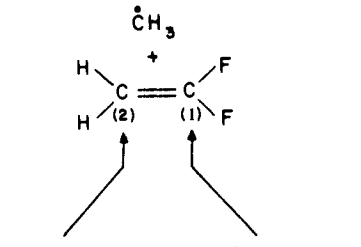

14a **14b**

collected. Indeed, $\Delta E°$ opposes the spin density effect, and the reaction on C_1 is now pronouncely more exergonic than on C_2. Thus, the moderate regiochemical preference in **14** arises from opposition of the two factors which is won by the spin-density effect. Our 3-21G results are similar to the 4-31G ones by Olivella et al.,[8b,c] and our $\Delta E°$ values show even a greater difference, being −19.7 for the C_2 attack vs −30.8 kcal/mol for the C_1 attack, while the corresponding $\Delta E^‡$ values are 9.1 and 9.8 kcal/mol, respectively.

The barrier constituents in **14a** vs **14b** behave as expected. Thus, the net higher ΔE_c for **14b** arises from a larger ΔE_{dis}. This fact is manifested as expected in the geometries of the corresponding TS's in **15a** vs **15b**.[8c]

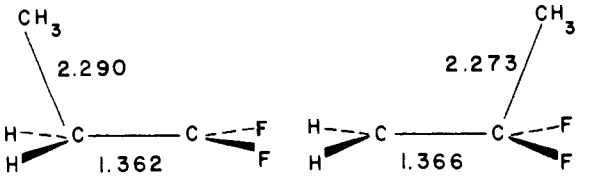

15a **15b**

At some point, the opposition of the spin density and $\Delta E°$ effects may balance out and eventually invert their importance to produce an "abnormal" regiochemistry. The reaction of $CF_2=CHF$ is a case in point. This olefin is known to give zero regioselectivity with CH_2Cl and an "abnormal" one with CH_3, while a "normal" regioselectivity is obtained with H, CF_3, and CCl_3.[2a]

Inspection of Table I shows that the spin-density difference in $CF_2=CHF$ is slight. Therefore a strong opposition of $\Delta E°$ can easily tip the balance toward an "abnormal" regioselectivity. This all depends on the bond strength differences in the two radical products. Drawing **16** shows these differences with use of bond energies of model compounds.[29d,e] Thus, when the radical is CH_3, $\Delta E°$ is expected to be ~10 kcal/mol more exergonic for attack on C_2 (CF_2 terminus) than on C_1. However, for radicals like H and CF_3 the $\Delta E°$ should possess a very small directive preference, if at all.

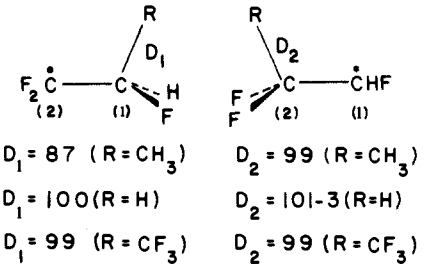

16

The reaction with CH_3 has been computed with the 3-21G basis set,[3] and the results, in terms of the usual quantities, are displayed in **17a** vs **17b**. It is seen that $\Delta E°$ is computed to be ~10 kcal/mol more exergonic for a C_1 attack. This large difference now opposes a small directive power of the higher spin density on C_2 (Table I). The result is a tiny preferrence for a C_1 attack, **17a**.

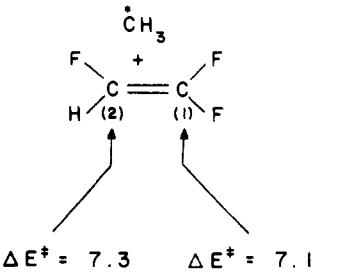

17a **17b**

Further inspection of **17a** vs **17b** shows that the ΔE_c quantities are indeed very close and reflect the opposition. Thus, ΔE_{dis} still shows that attack on C_1 requires more distortion to localize the electron on the union center. On the other hand, the $\Delta E°$ effect requires less ΔE_{rep} for a C_2 attack which coincides with a larger $CH_3\cdots C$ distance in the corresponding transition state, **18b** vs **18a**.

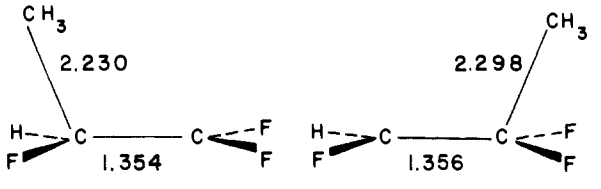

18a **18b**

Clearly, as the radical is varied from CH_3 to H or CF_3, the $\Delta E°$ directive effect is diminished, and the spin-density effect will take over to restore the normal regioselectivity of a C_2 attack (at the CHF terminus).

The principles of regioselectivity are therefore quite simple and can be used to make some verifiable predictions. Thus, for example, Cl is a bond-weakening substituent, unlike F. One may therefore anticipate that in $Cl_2C=CHCl$ all radicals will have a slightly weaker bond with the CCl_2 terminus. As a result, the spin-density effect is expected to dominate and direct the regiochemistry always toward the less substituted terminus.

III. Summary

We have used here the SCD model to derive regiochemical patterns in the radical addition to olefins. Regiochemistry can be discussed in terms of two factors which are related to fundamental properties of the radical and the olefin. The first factor is the relative spin density in the $^3\pi\pi^*$ state of the olefin. *This factor directs the regiochemistry toward the spin-rich olefinic carbon.* The second factor is the bond strength of the radical to the olefinic carbon. *This factor directs the regiochemistry toward*

the olefinic terminus which forms the strongest bond with the radical.

Regioselectivity is the net result of these two effects. When they join up regioselectivity will be large. When they oppose one another, regioselectivity will be smaller, and regioselectivity crossovers are expected. In most cases known to us, the spin-density effect wins over. The relative spin densities are found to parallel the relative HOMO coefficients of the olefin. Therefore the predictions of the spin-density effect an the HOMO-rule[6] will normally be identical. The ΔE_{dis} quantity is also usually a reliable regioselectivity index, and the smaller ΔE_{dis} usually coincides with the spin-rich site.

The role of "steric effects" cannot be ruled out. The way we define "steric effect" is that this is the specific contribution to the exchange repulsion between the electrons of the substituent and those of the radical. With this definition, "steric effect" is part of the ΔE_{rep} term (eq 2). As may be seen, ΔE_{rep} is usually, though not always, larger for the attack on the more substituted site.

Thus, in many cases all the regioselectivity indexes will coincide and reflect the total destabilization, ΔE_c, which the reactants have to undergo in order to achieve resonance with the excited states, Ψ^*_{RP}, in the diagram in Figure 1. It is then the integrated index ΔE_c ($\Delta E_c = \Delta E_{dis} + \Delta E_{rep}$) which will make the more successful predictions and is, itself, predictable by the balance of the spin density and bond strength effects.

Registry No. CH_2=CHX (X = Ph), 100-42-5; H_2C=CHF, 75-02-5; H_2C=CF_2, 75-38-7; FHC=CF_2, 359-11-5; H_2C=CHCl, 75-01-4; ClHC=CF_2, 359-10-4; H_2C=$CHCH_3$, 115-07-1; H_2C=$CHCF_3$, 677-21-4; H_2C=CHCN, 107-13-1; H_2C=CHCH=CH_2, 106-99-0; H_2C=$CHNH_2$, 593-67-9.

The Role of Intramolecular Hydrogen Bonding as a Determinant of the Conformational Profiles of cGMP and cAMP

Sid Topiol,*,† Thomas K. Morgan, Jr.,* Michael Sabio, and William C. Lumma, Jr.

Contribution from the Department of Medicinal Chemistry, Berlex Laboratories, Inc., Cedar Knolls, New Jersey 07927. *Received March 2, 1989*

Abstract: Computational chemical studies using the AM1 semiempirical method and Hartree–Fock calculations with the STO-3G basis set using the AM1 structures have been performed on the cyclic nucleotides adenosine 3′,5′-cyclic monophosphate (cAMP), guanosine 3′,5′-cyclic monophosphate (cGMP), and model compounds. Consistent with earlier experimental and computational studies, cGMP is expected to prefer the syn conformation of the purine/sugar portions, while cAMP prefers the anti conformation. The present studies implicate an intramolecular hydrogen bond, between a hydrogen atom of the C2-amine of the purine and the axial oxygen atom of the cyclic phosphate, in increasing the relative stability of the syn conformation of cGMP. Analysis of the energetics and molecular electrostatic potentials of model compounds and model complexes reveals that the substituent at the C6 carbon atom and the phosphate ring conformation play critical roles in stabilizing this interaction. These conformational profiles along with tautomeric characteristics may help develop hypotheses to explain selectivity for binding to and activation of proteins by the cyclic nucleotides.

The cyclic nucleotides guanosine 3′,5′-cyclic monophosphate (cGMP) and adenosine 3′,5′-cyclic monophosphate (cAMP) (Figures 1 and 2) play central roles in many biochemical processes. Both serve as second messengers in diverse receptor mediated events. Insights into the mechanisms of interaction of these cyclic nucleotides as ligands for cGMP or cAMP dependent protein kinases (PKs) or as substrates for phosphodiesterases (PDEs) can be obtained through various routes. For instance, with use of the crystal structure of catabolite gene activator protein[1] (CAP) bound with cAMP together with sequence homologies between CAP and cAMP dependent protein kinase C (PKc), Weber et al.[2] have recently proposed a model for the structure of the cAMP binding site of PKc. In a similar fashion, modeling studies together with protein sequence and structural data have been synthesized to generate models for cGMP and cAMP dependent PDE.[3] Alternatively, Wells et al.[4] have developed a model for cGMP versus cAMP dependent PDEs based on an analysis of structure activity relationships of ligands for these enzymes. More recently, Erhardt and co-workers used structure activity relationships to develop a model for the cardiac cAMP PDE catalytic site.[5] Computational studies of the physicochemical properties of these isolated species have also been performed.[6,7] These physicochemical studies can be used to develop mechanistic models either independently or in conjunction with models developed through other means as described above. The present study represents the first of our computational studies on the physical chemical properties of cGMP and cAMP related compounds. In a separate paper,[8] we report the tautomeric properties of adenine and guanine. We focus herein on the conformational properties of cGMP and cAMP, and related models as these are salient features of existing models for their activity (e.g., ref 2 and 3).

Methods

The structures of the parent compounds cGMP, cAMP, and various analogues (defined herein) were fully optimized (unless otherwise indicated) by the use of the semiempirical AM1 method[9] as implemented in

† Present address: Sandoz Research Institute, East Hanover, NJ 07936.

(1) (a) McKay, D. B.; Steitz, T. A. *Nature* **1981**, *290*, 744. (b) McKay, D. B.; Weber, I. T.; Steitz, T. A. *J. Biol. Chem.* **1982**, *257*, 9518.
(2) Weber, I. T.; Steitz, T. A.; Bubis, J.; Taylor, S. S. *Biochemistry* **1987**, *26*, 343.
(3) Topiol, S.; Sabio, M. Computational Studies of Ligand/Receptor Interactions. In *Computer-Assisted Modeling of Receptor-Ligand Interactions: Theoretical Aspects and Applications to Drug Design*; Golembek, A., Rein, R., Eds.; Alan R. Liss: New York, 1989 pp 455–464; also, unpublished results.
(4) Wells, J. N.; Garst, J. E.; Kramer, G. L. *J. Med. Chem.* **1981**, *24*, 954.
(5) Erhardt, P. W.; Hagedorn III, A. A.; Sabio, M. *Mol. Pharmacol.* **1988**, *33*, 1.
(6) Davis, A.; Warrington, B. H.; Vinter, J. G. *J. Comput.-Aided Mol. Design* **1987**, *1*, 97.
(7) Yathindra, N.; Sundaralingham, M. *Biochem. Biophys. Res. Commun.* **1974**, *56*, 119.
(8) Sabio, M.; Topiol, S.; Lumma, W. C., Jr. *J. Phys. Chem.* In press.

0002-7863/90/1512-1452$02.50/0